

Reply to Reviewer Comments – T Smith et al.

W. Guo – General Comments

1. The authors provide some comparisons with previous studies on the classification of debris covered glaciers. Although it seems enough for describe the improvements made by the algorithm presented in this manuscript, it would be better to give some direct comparisons on which kinds of area were committed or omitted by the authors' method or by other methods, because the descriptions of those methods can mostly be easily followed and applied in the study region or even in a small region. This kind work can show more details on the improvements made by this paper, and further promote the scientific significance of this paper. However, this is totally depending on the authors' choice.

It was outside the scope of this study to re-code previous algorithms for direct comparison. During the development of our algorithm, we tested methods from several previously published algorithms before developing our final product. However, without the original proprietary software packages, ground control points, and spectral thresholds tuned to specific scenes which were used in several of the methods, we did not feel it was appropriate to make a direct comparison between the results of our algorithm and the results of previous work. We have aimed with this manuscript to rely as much as possible on open-source tools and to develop an algorithm which is not specifically tuned to a single Landsat scene footprint or set of spectral thresholds.

In light of the comments of both reviewers, however, we have attempted to recreate the algorithm used by Paul et al. (2004) in a simple Matlab implementation. We have found that the neighborhood analysis, as performed with a neighborhood filter, is very computationally expensive. It is likely that the Image Polygon Growing algorithm included with the software package PCI is a more efficient implementation of a similar analysis, but the authors could not find a fast implementation of this analysis. Despite computational issues, the approach did not show strong improvements over the methods proposed in our algorithm. An overlay of our final outlines and the outlines created using the TM4/5 >2, HIS > 126, and Slope > 24, along with the neighborhood analysis is included in this reply as Figure 1.

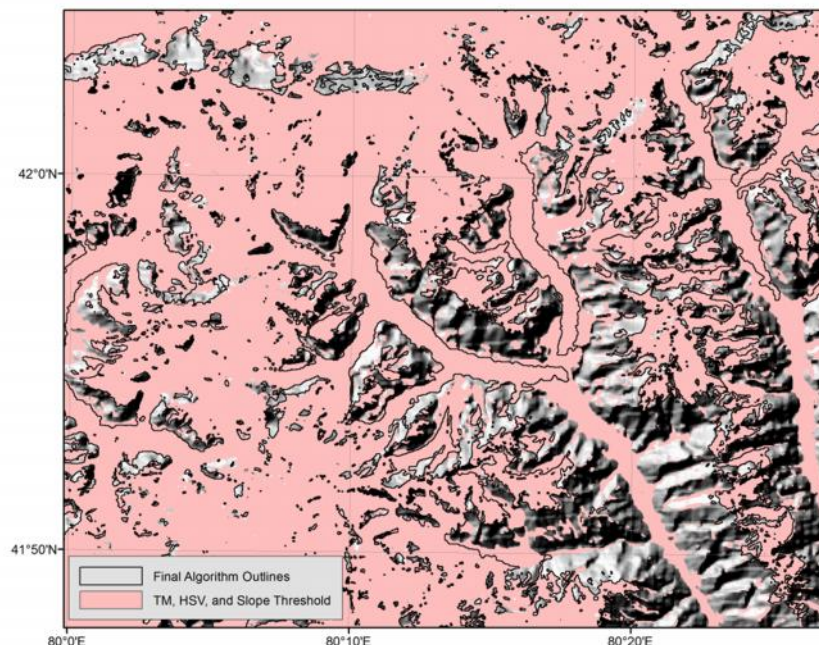


Figure 1: Final algorithm outlines (black) as compared to TM, HSV, and Slope threshold (red).

In our study area, we find that most debris-covered glacier tongues are connected to long trails of debris, misclassified river sand, and glaciers, and the neighborhood analysis has difficulty removing these areas. In Figure 1 we see our algorithm outlines overlain with the results of the TM, HSV, and Slope thresholding in red. Despite the promising approach of neighborhood analysis, we did not see significant improvement in our study region, so we did not include this method in our algorithm.

2. From my view, too many figures were used in the new version manuscript (totally 15). Some of them, which belong to same groups (like Figure 2-8 that describe the processing steps, and Figure 10-12 that illustrate the elevation distribution of glaciers and their comparison to other glacier outlines), can be merged into one figure (mark as a, b, c, etc). Some of the figure captions can also be simplified and shortened, leave the descriptive words in main text. Besides, the acquisition date for Landsat images shown as background in Figure 2, 5-8, 14, 15 should better to be explicitly marked on the figure, or described in the caption, for the conveniences of reader's check.

We have modified the figures as-per the comments of both reviewers to minimize the number of figures.

3. Although the authors have done very hard works and processed large number of Landsat scenes (totally 62), it is difficult to find the related results in the Results and Discussion section (they only describe some comparisons with existing glacier inventories, and the manual control dataset created by authors that around 2000 and 2011) for most scenes. From my view, the number of Landsat scenes processed is not important comparing to the efficiency and accuracy of the algorithm. So I suggest that the author revise the data source section and shorten the Table 1, only keep the Landsat scenes whose results were introduced in the Results and Discussion section.

We have updated the table to only include those scenes explicitly used in the manuscript. This includes scenes used as 'master' references, those used for velocity profile generation, and those used for the glacier statistics. We have also included all scenes for path-row combination 147/31, as these were all used in the discussion of factors that degrade algorithm outputs (snow, clouds, etc).

W. Guo – Specific Comments

Line 7: The citations for the data and following paper are both needed for the second Chinese glacier inventory (for here and also other places).

Guo, W., Liu, S., Xu, J., Wu, L., Shangguan, D., Yao, X., Wei, J., Bao W., Yu, P., Liu, Q., and Jiang, Z.: The second Chinese glacier inventory: data, methods and results, J. Glaciol., 226, 957-969, doi: 10.3189/2015JoG14J209, 2015.

This has been updated.

Line 13: “~1-2 pixels of Landsat Enhanced Thematic Mapper ...”, it is necessary to mention the panchromatic band of Landsat ETM+;

This has been updated

Line 17: “multi-spectral” is better here.

This has been updated.

Line 43-46: there's no nation name in Figure 1, so it is inconvenient to readers with less knowledges on Central Asia. The WWD and Siberian High also with same situations. See comment on Figure 1.

This has been updated.

Line 111: “spectrally-derived”, maybe a further description should better to be presented here (I mean clean-ice, maybe in parenthesis).

This has been updated.

Line 120-123: how the elevation threshold of low elevation area was determined? Is it determined by subtract certain value from the average value of clean-ice areas? It should also to be clarified here.

To find the low elevation threshold, we subtract 1750 from the average elevation of clean-ice areas. This has been clarified in the manuscript.

Line 207: “as well as both clean and debris-covered”, “clean-ice” is better here.

This has been updated.

Line 262-272: Although the normalized distances can show the general distribution of the bias along the glacier outline, it should be better to give some summaries on the common statistics of the vertex biases, like the maximum and mean distance of all validated vertex pairs. Besides, how the distances were normalized also need more details, e.g., were all distances normalized to one maximum distance? Or different glaciers have different maximum distances? If the first case, what is the maximum distance of all vertex pairs? Without such details, the normalized distances have very less sense on describe the vertex distance distribution. Also see comments on Figure 13.

The distances were normalized by the spread of the min and max values of the vertices, with the formula $(\text{Distance} - \min(\text{Distance})) / (\max(\text{Distance}) - \min(\text{Distance}))$, with the y axis plotted as a percentage of the maximum normalized distance, as the spread of values between algorithm and clean-ice results is quite different. The minimum distance for both datasets is 15, with the maximum for the algorithm at 46,000 and clean-ice at 23,000. These distant points represent outliers, and comprise points very far removed from the actual glacier outline. This discussion has been added to the manuscript.

Line 285: Generally the configuration of the computer (e.g., CPU, physical memory, operating system) need to be provided if you give a processing time.

The data was processed on Ubuntu 14.04, 8 cores (3.6GHz), 16 GB RAM. This has been added to the manuscript.

Table 1: The data source should better to be simplified and shortened, leaves only the images whose results were shown in the Results and Discussion section.

We have shortened and simplified this data table.

Figure 1: From common sense, it is better to show the nation names on the map, maybe by showing the national boundaries and names in the main map. Besides, the Winter Westerly Disturbances (WWD) and the Siberian High are also need to be shown on the map, maybe by labelled arrows.

This has been updated.

Figure 2-8: these figures can be merged into one figure and marked as a), b), c), d), etc, corresponding to the processing step. The figure captions should also be shortened and simplified.

We have modified the figures and captions.

Figure 10-12: these three figures can also be merged into on figure which shows the elevation distribution of the algorithm extracted glaciers and their comparisons to other source of glacier outlines (spectral, manual and CGI V2).

We have combined these figures.

Figure 13: It is suggested to give more details on the distances of all validated vertex pairs, like the maximum and mean distances of all validated vertex pairs if all distances were normalized to one maximum distance, or maximum and mean distances of each glacier if different glaciers have different maximum distances.

This has been updated in the manuscript. See as well a more detailed reply above.

F. Paul – General Comments

The revised study by Smith et al. is now much more focused and provides a thorough description of the developed algorithm and its performance compared to other datasets. Considering earlier versions of the ms, I think this reduction had really been beneficial. The authors have also further modified the computational part towards a more automated processing line, thus facilitating its application to other regions. Although they used constant thresholds for the band ratio result in a reduced accuracy of the outlines in the accumulation region (e.g. missed ice in shadow), the improved mapping of debris-covered glacier tongues seems worth applying the method. My only larger recommendation is to also include a comparison of the results of the method presented here to results from other simple approaches (e.g. Nr. 2 and 5 in Table 2). This would help to see whether the calculation of velocity fields beforehand is worth the effort or not. As now clearly stated, it has also to be considered that the results of the algorithm require improvement when working at the scale of individual glaciers, but might satisfy the needs for regional scale applications. Apart from the comparison mentioned above, I have only some smaller comments that are detailed in the next section. Once these are addressed I am happy to recommend acceptance of the ms.

It was outside the scope of this study to re-code previous algorithms for direct comparison. During the development of our algorithm, we tested methods from several previously published algorithms before developing our final product. However, without the original proprietary software packages, ground control points, and spectral thresholds tuned to specific scenes which were used in several of the methods, we did not feel it was appropriate to make a direct comparison between the results of our algorithm and the results of previous work. We have re-coded in our development parts of previous algorithms, which were used in the development of our final product (see above).

F. Paul – Specific Comments

Title and overall remark

Please use glacier / glacierized instead of glacial/glaciated when reference is made to contemporary glaciers. The title should thus be “Improving semi-automated glacier mapping ...”

This has been updated.

Abstract first sentence

I suggest rewriting the first sentence a little bit: "Studies of glaciers generally require precise glacier outlines. Where these are not available, extensive manual ... (GIS) must be performed, as current ..."

This has been updated.

L5 The dataset is "known as the Randolph Glacier Inventory"

This has been updated.

L11: Please cite here the Cryosphere Chapter (Vaughan et al. 2013) instead of the full report (Stocker 2013).

This has been updated.

L43: I would recommend to not introducing here a further abbreviation (WWD), also because it is not used any further.

This has been updated.

L58: Please add the method used for downsampling (bilinear interpolation?).

This was already found in the manuscript at L59: *"The SRTM data and its derivatives were downsampled to 30 m to match the resolution of the Landsat images using bilinear resampling."* We have maintained this as-is.

L58: Here and elsewhere (e.g. L59, L96, L99): Please insert a space between the value and the unit (30 m).

This has been modified throughout the manuscript.

L74ff: As Matlab is proprietary software, it would be most useful to establish also for the glacier classification steps scripts written in Python or other free software (see L100/1). Maybe this can already be achieved for the final version of the ms?

We have attempted to move all of our processing to Python, but still rely on a distance weighting algorithm built in Matlab which does not have a good implementation in Python. Once a suitable alternative to the current distance weighting metric is developed, we will shift all of our code to Python.

L92: Hanshaw and Bookhagen, here and elsewhere (e.g. L109): Please cite this study only when it is accepted for TC.

This study has been published. We have updated the citation to reflect this.

L109: Hall et al. (1987) applied the TM4/TM5 band ratio for glacier mapping first. The TM3/TM5 ratio combined with a TM1 threshold was introduced by Paul and Kääb (2005).

This citation has been added.

L111: I suggest inserting here a comment on its general use: For normal the two thresholds are adjusted manually to the image conditions of each individual scene to obtain the best results. When the automated

processing line is based on constant thresholds, large errors can occur in regions of cast shadow (see also example in Paul et al. 2015).

We have added this comment and citation.

L128, 248 and elsewhere: Instead of 'glacier debris tongue' I would write 'debris-covered glacier tongue'.

This has been modified throughout the manuscript.

L145: As there is always snow on-glaciers and clouds off-glaciers do not matter, I would write here more precisely: "It is important to note that images must be cloud free over glaciers and snow free off-glaciers for this step."

This has been updated.

L182: I can imagine that this step is as efficient as the neighbourhood analysis used by Paul et al. (2004): Everything that is not connected to a glacier is removed. I suggest to shortly explaining what the differences in performance are.

The two methods are similarly efficient over small areas, but start to diverge in processing time as the number of individual 'seed' areas increases. For example, the geodesic distance algorithm we use operates on a whole-matrix basis, and is quite fast regardless of the number of seed points. The neighborhood analysis, which treats individual areas as separate objects to check connectivity with, requires more intense processing as the number of areas increases. The geodesic time algorithm also imposes a limit on the size of the areas connected to a glacier, so if a long trail of river sand, for example, is connected to a glacier the entirety of this area is not included as a connected component. Rather, only the pixels which are 'close' to the glacier are kept as debris areas. We have added a note in this section of the manuscript regarding the differences.

L195: What about using neighbourhood analysis instead? A gap that is completely surrounded by debris is assigned to the debris class given its slope is below a certain threshold. This would likely fill gaps of any size within the debris.

A neighborhood analysis was tested for this step and found to be processor-intensive, especially when there are often tens of thousands of small 'holes' in glacier areas which must be checked and filled. We find that the bridging and void-filling tools work well without applying a neighborhood analysis, but future iterations of the algorithm could include this step as an option.

L205 & 363: path-row combinations

This has been updated.

L214: The void-filled SRTM DEM is in some mountain ranges with steep topography of very poor quality (where the voids had been filled). Has this not caused any trouble in the regions analysed here?

We are aware of the issues surrounding the SRTM DEM at high elevations. However, for this analysis, we use watersheds as convenient polygons to divide glaciers into individually comparable areas. Thus, if there is a small error in the watershed boundary, that error is the same throughout the analysis and statistical comparison, and should not impact our statistics. We also manually checked and updated our watershed boundaries for any major errors.

L218: If possible I suggest adding a section for a glacier-by-glacier comparison of glacier area. The elevation related statistics are fine (please consider showing elevation on the yaxis for Figs. 10 to 12), but the standard deviation of the area differences would be most useful when it comes to using the algorithm for regional-scale change assessment.

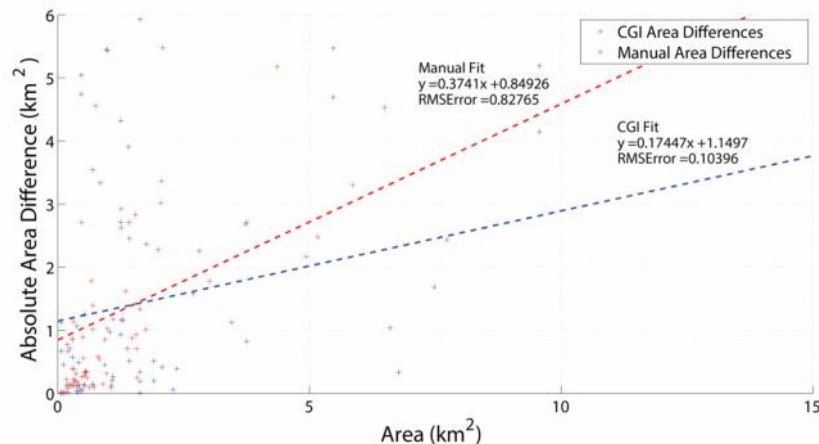


Figure 2: Glacier Area vs Area misclassification, as compared to both a subset of the manual control dataset and the CGI

From our reply to the previous round of reviews: “We have included in this reply a plot illustrating the differences in classification across different size classes, which can be seen in Figure 2. We emphasize, however, that the algorithm was not designed around mapping individual glacier areas, and such a comparison was removed from the original version of the manuscript. As a slight change in which areas are ‘connected’ by snow, misclassified pixels, or other classification issues can drastically change the reported glacier area, we do not present this data in the updated manuscript. If, for example, a glacier with an area of 10 sq km was connected by a small strip of misclassified area to a glacier of 50 sq km, the reported area would be 60 sq km, which matches poorly if it is compared to either the 10 sq km or 50 sq km glacier area. As this creates a large number of outliers for individual glacier comparisons, we have elected not to present individual-level glacier statistics in the revised manuscript.”

We maintain that our algorithm is most useful for large-scale analyses, and the analysis of individual glaciers is better completed using manually digitized outlines, or a manual correction of our final algorithm output.

L219: over two distinct

This has been updated.

L224-226: I suggest numbering these three comparisons (e.g. (a), (b), (c)) for a more easy reference and recognition later on.

We have opted to leave this section as-is, as we have combined the three figures which use these comparisons into a single figure, simplifying this discussion.

L232: When I look at the primary (spectral) classification in Figs. 2 and 8, I would argue that the difference is due to the not-mapped ice in shadow for many of the north-facing small glaciers. A lower TM1 threshold would have helped to include these regions. Please rewrite if this is agreeable.

Shadows are certainly part of the issue, both at high- and low-elevations. However, as you have pointed out, there are some major exclusions at mid- to low-elevations due to shadows. We have added a sentence reflecting this.

L237: It could also be well the case that the CGIv2 under-classifies these regions.

Yes, this is possible as well. We have chosen to leave the text as-is, as we only analyze relative differences. The distinction between underclassification/overclassification is only a matter of which dataset is chosen as the 'master' dataset.

L252: Though correct, I think it is rather obvious that a method that also maps the debris covered part will be better than a pure spectral classification. A more interesting comparison would be against one of the other methods summarized in Table 2. Can this be done for a sub-region? After all, it is still not clear whether the higher workload required for this method is worth the effort compared to more simple approaches (e.g. Nr. 2 or 5 in Table 2).

We have included in this reply an implementation and discussion of the Paul et al. (2004) algorithm, which can be seen in Figure 1.

L264: What are 'component vertices'? Can the method be described in somewhat more detail?

Component vertices are simply the set of every vertex of our glacier polygons. We then use the set of X/Y pairs for each vertex to compare to the X/Y pairs of the vertices of the clean-ice and final algorithm polygons. We have expanded our description in the manuscript.

L287: Here I disagree a little bit, the neighbourhood analysis is an implemented routine and very quick. The entire processing line described in Paul et al. (2004) also only takes a couple of minutes. This is also the reason why I have suggested above a comparison of results to other 'more simple' methods.

The neighborhood analysis, as implemented in Matlab, is significantly slower than our algorithm. In tests on our desktop computer, the single step of neighborhood filtering takes more time than the entire algorithm run-through, including the conversion of the end result geotiff to a complex vector file. It is likely that a more efficient implementation of this neighborhood analysis could be performed using a combination of proprietary software and FORTRAN, as proposed by Paul et al. (2004), but this was outside the scope of this study. An efficient neighborhood analysis could be included in subsequent versions of the algorithm, if a Matlab or open-source version could be implemented.

L311: between terrain on and off glaciers

This has been updated.

L332: debris-covered glacier tongues ... centre

This has been updated.

L347: analysing?

This has been changed.

L347: “powerful tool”: I well see the potential of the method, but think that its real test comes when applying it to the often slow moving or even stagnant debris-covered tongues in the Himalaya. I suggest adding this information here.

We have added this caveat to the manuscript.

L446: Kaab should be Kääb; L450: Bris, R. L. should be Le Bris, R.

L487: Stocker, D.Q. should be Stocker, T. (but please replace with Vaughan, D.G.)

These have been updated.

Tables

Table 1: I suggest writing “Landsat acquisition dates” (in the caption and the left column)

This has been updated.

Table 2: The Paul et al. (2004) method was actually applied to a Landsat full scene (33,000 km²), but results were only presented for a sub-region to see something.

In this table we present the total mapped *glacier* area of each study, as opposed to the area of the entire study site. As the classification/misclassification statistics presented in Paul et al. (2004) refer to the subset glacier area, we will maintain the table as-is. If there are more accurate statistics on the total mapped glacier area and misclassification percentages, we would be happy to include these values in the manuscript.

Figures

Fig. 1: Please add location of sub-regions in Fig. 1.

This has been updated.

Fig. 2: Please indicate where the debris-covered tongues are (arrow, circle)

This has been updated.

Fig. 3: Has the slope map already been median filtered? If not, maybe do it.

We have added this step to the algorithm, but do not see significant changes to our classification.

Fig. 3 & 4: I suggest adding the outlines from Fig. 2 on top to see the differences.

We have updated these figures.

Fig. 6: For better visibility I suggest using yellow instead of red.

We have changed this color scheme.

Figs. 11 to 13: The caption already includes a substantial amount of interpretation (last sentence). I suggest removing this here and provide the information in the main text.

We have updated our figure captions.

Figs. 14 and 15: Please use different colours for the lines. I suggest the red one could be yellow and the purple one white. Maybe add arrows to highlight discussed features.

We have changed the colors to be more visible. Bright yellow and white are difficult to see on many of the bright, high-elevation glacier areas, but we have attempted to make the outlines more visible.

T. Bolch – Specific Comments

L. 120: I agree that slope is one key morphometric parameter for delineating the debris-covered areas. However, the suggested threshold values differ depending on glacier type from the 24° suggested by for Oberaletschgletscher/Swiss Alps (Paul et al. 2004), for example, it is 12° for Khumbu Glacier/Himalayas (Bolch et al. 2007), less than 15° for Samudra Tapu Glacier/Himachal Himalayas (Shukla et al. 2010) and 18° for Gangotri Glacier/Garhwal Himalayas (Bhambri et al. 2011). Maybe you could check your chosen threshold (just a suggestion), but please provide some info about the different suggested thresholds here or in the discussion.

This is a very good point. We choose a conservative slope threshold to ensure that we do not remove debris-covered areas in this initial step, and instead rely on subsequent steps to remove overclassified areas. We have added a discussion of these citations and our reasoning behind using the 24 degree threshold suggested by Paul et al. (2004).

L. 275: Be a bit more specific about the 6 cited references. You may (but not must) include Bhambri et al. (2011), IJRS who also clearly mention the limitations of their approach.

We have opted to include the Bhambri et al. (2011) study in Table 2. We have also clarified the references on L290.

Improving Semi-Automated Glacier Mapping with a Multi-Method Approach: Applications in Central Asia

Taylor Smith¹, Bodo Bookhagen¹, and Forest Cannon²

¹Institute for Earth and Environmental Sciences, Universität Potsdam, Germany

²Geography Department, University of California, Santa Barbara, USA

Corresponding ~~author~~^{author}:

Taylor Smith ~~and Bodo Bookhagen~~

Institute for Earth and Environmental Sciences

Universität Potsdam

Potsdam-Golm 14476, Germany

Email: tsmith@uni-potsdam.de , ~~bodo@geo.uni-potsdam.de~~

Abstract.

Studies of glaciers ~~often require~~ generally require precise glacier outlines. Where these are not available, extensive manual digitization in a Geographic Information System (GIS) must be performed, as current algorithms struggle to delineate glacier areas with debris cover or other irregular spectral profiles. Although several approaches have improved upon spectral band ratio delineation of glacier areas, none have entered wide use due to complexity or computational intensity.

In this study, we present and apply a glacier mapping algorithm in Central Asia which delineates both clean glacier ice and debris-covered glacier tongues. The algorithm is built around the unique velocity and topographic characteristics of glaciers, and further leverages spectral and spatial relationship data. We found that the algorithm misclassifies between 2 and 10% of glacier areas, as compared to a ~ 750 glacier control dataset, and can reliably classify a given Landsat scene in 3-5 minutes.

The algorithm does not completely solve the difficulties inherent in classifying glacier areas from remotely sensed imagery, but does represent a significant improvement over purely spectral-based classification schemes, such as the band ratio of Landsat 7 bands three and five or the Normalized Difference Snow Index. The main caveats of the algorithm are (1) classification errors at an individual glacier level, (2) reliance on manual intervention to separate connected glacier areas, and (3) dependence on fidelity of the input Landsat data.

1 Introduction

This study focuses on mapping glaciers over a large spatial scale using publicly available remotely sensed data. Several high-resolution glacier outline databases have been produced, most notably the Global Land Ice Measurements from Space (GLIMS) project (Armstrong et al., 2005; Raup et al., 2007, 2014), and the recently produced supplemental GLIMS dataset known as the Randolph ~~Glacial~~ Glacier Inventory (RGI) v4.0 (Arendt et al., 2012; Pfeffer et al., 2014). Smaller-scale glacier databases are also available, such as the Chinese Glacier Inventory (CGI) v2 (Guo et al., 2015). A coherent, complete, and accurate global glacier database is important for several reasons, including monitoring global glacier changes driven by climate change, natural hazard detection and assessment, and analysis of the role of glaciers in natural and built environments, including glacier contributions to regional water budgets and hydrologic cycles (Racoviteanu et al., 2009; Vaughan et al., 2013). Precision in glacier outlines is of utmost importance for monitoring changes in glaciers, which may change less than 15-30 m/yr (~ 1 -2 pixels of Landsat Enhanced Thematic Mapper (ETM+) Panchromatic band/yr). ~~Thus, spatially accurate glacier outlines are imperative for precise glacier change detection (Paul et al., 2004, 2013).~~

Several methods have been developed to delineate clean glacier ice (i.e. Hall et al., 1987; Paul, 2002; Paul et al., 2002; Racoviteanu et al., 2008a,b; Hanshaw and Bookhagen, 2014), relying primarily on ~~spectral data available on~~ multi-spectral data from satellites such as Landsat and Advanced Spaceborne Thermal Emission and Reflection Radiometer (ASTER). Although significant progress has been made towards automated glacier outline retrieval using satellite imagery, these methods struggle to accurately map debris-covered glaciers, or other glaciers with irregular spectral profiles (~~Paul et al., 2004; Bolch et al., 2007; Racoviteanu et al., 2008b; Scherler et al., 2011a~~) (Paul et al., 2004; Bolch et al., 2007; Racoviteanu et al., 2008a,b; Scherler et al., 2011a). Much of this difficulty stems from the similarities in spectral profiles of debris located on top of a glacier tongue and the surrounding landscape. The majority of studies examining debris-covered glaciers employ extensive manual digitization in a Geographic Information System (GIS), which is very time consuming, and can introduce significant user-generated errors (Paul et al., 2013; Pfeffer et al., 2014; Raup et al., 2014). Building on the multi-spectral, topographic, and spatially-weighted methods developed by Paul et al. (2004), we present a refined rules-based classification algorithm based on spectral, topographic, velocity, and spatial relationships between glacier areas and the surrounding environment. The algorithm has been designed to be user-friendly, globally applicable, and built upon open-source tools.

2 Study Area and Data Sources

2.1 Study Area

In this study we ~~use~~ analyze the results of our classification algorithm using a suite of ~~62-40~~ Landsat
35 Thematic Mapper (TM), Enhanced Thematic Mapper+ (ETM+) and Optical Land Imager (OLI)
images (1998-2013) across a spatially and topographically diverse set of study sites comprising
eight Landsat footprints (Path/Row combinations: 144/30, 145/30, 147/31, 148/31, 149/31, 151/33,
152/32, 153/33) along a $\sim 1,500$ km profile from the Central Pamir to the Central and Central-Eastern
Tien Shan (Figure 1, Table 1) ~~to analyze the results of our classification algorithm.~~

40 The study area contains a wide range of glacier types and elevations, with both small and clean-
ice dominated glaciers, as well as large, low-slope, and debris-covered glaciers. The diversity in
glacier types in the region provides an ideal test area ~~for~~ particularly in mapping glaciers with long
and irregular debris tongues, such as the Inylchek and Tomur glaciers in the Central Tien Shan
(Shangguan et al., 2015).

45 The wintertime climate of the study area is controlled by both the Winter Westerly Disturbances
(~~WWDs~~) and the Siberian High, which dominate regional circulation and create strong precipitation
gradients throughout the range, which extends from Uzbekistan in the west through China in the
east (Figure 1) (Lioubimtseva and Henebry, 2009; Narama et al., 2010; Bolch et al., 2011; Sorg
et al., 2012; Cannon et al., 2014). The western edges of the region tend to receive more winter
50 precipitation in the form of snow, with precipitation concentrated in the spring and summer in the
central and eastern reaches of the range (Narama et al., 2010).

2.2 Data Sources

Our glacier mapping algorithm is based on several datasets. The Landsat 5 (TM), 7 (ETM+), and
8 (OLI) platforms were chosen as the primary spectral data sources, as they provide spatially and
55 temporally extensive coverage of the study area (Table 1). ASTER can also be used as a source of
spectral information, but here we chose to focus on the larger footprint and longer timeseries avail-
able through the Landsat archive. In addition to spectral data, the 2000 Shuttle Radar Topography
Mission V4.1 (SRTM) Digital Elevation Model (DEM) (~~$\sim 90\text{m}$~~ 90m , void-filled) was leveraged to
provide elevation and slope information (Jarvis et al., 2008). The SRTM data and its derivatives
60 were downsampled to ~~30m~~ 30m to match the resolution of the Landsat images using bilinear resam-

pling. The USGS Hydrosheds river network (15 second resolution, $\sim 500\text{m}$) was also used as an input dataset (Lehner et al., 2008).

3 Methods

Our glacier classification algorithm uses several sequential thresholding steps to delineate glacier outlines. The scripts used in this study are available in the Data Repository, with updates posted to <http://github.com/ttsmith89/GlacierExtraction/>. It is noted if the step requires manual processing or is part of a script.

1. Data Pre-processing

- (a) Velocity fields are calculated with Normalized Image Cross Correlation (Manual, can be automatized)
- (b) The Hydrosheds river network is rasterized (Manual, can be automatized)
- (c) Optional manual debris points are created (Manual, optional)
- (d) SRTM data is used to create a hillslope image (Python Script)
- (e) All input datasets are matched to a single extent and spatial resolution (30m) (Python Script)

2. Glacier Classification Steps

- (a) Clean-ice glacier outlines are created using Landsat Bands 1,3, and 5 (Matlab Script)
- (b) 'Potential debris areas' are generated from low-slope areas (Matlab Script)
- (c) Low-elevation areas are removed (Matlab Script)
- (d) Low-velocity areas are removed (Matlab Script)
- (e) Distance-weighting metrics are used to remove areas distant from river networks or clean glacier ice (Matlab Script)
- (f) Distance-weighting metrics are used to remove areas very distant from clean glacier ice and manual seed points (Matlab Script)
- (g) The resulting glacier outlines are cleaned with statistical filtering (Matlab Script)

3. Post-processing

- (a) Glacier outlines are exported to ESRI shapefile format for use in a GIS (Python Script)

3.1 Data Preparation

For accurate glacier delineation, we primarily used Landsat images which were free of new snow, and had less than 10% cloud cover. However, we have also included scenes with limited snow- and cloud-cover in our analysis to understand their impacts on our classification algorithm. We find that the presence of fresh snow in images tends to overclassify glacier areas and classify non-permanent snow as glaciers. Additionally, cloud covered glaciers cannot be correctly mapped by the algorithm (Paul et al., 2004; Hanshaw and Bookhagen, 2014). We use the USGS Level 1T orthorectified Landsat scenes to ensure that the derived glacier outlines are consistent in space (Hansen and Loveland, 2012; Nuimura et al., 2014).

The algorithm uses Landsat imagery, a void-filled DEM, a velocity surface derived from image cross-correlation, and the Hydrosheds 15s river network (buffered by ~~200m~~ 200 m and converted to a raster) as the primary inputs (Steps 1(a) and 1(b)). The algorithm generates a slope image from the DEM and rectifies additional input datasets described below for processing by resampling and reprojecting each dataset to the same spatial extent and resolution (~~30m~~ 30 m to match the Landsat data) (Steps 1(d) and 1(e)). Although the current algorithm leverages a few proprietary Matlab commands, we will continue to update the code with the goal of using only open-source tools and libraries in the future.

3.2 Clean Ice Delineation

Calculations are performed on rasterized versions of each input dataset, which have been standardized to the same matrix size. The first step in the classification process leverages Landsat 7 Bands 1, 3, and 5 (Step 2(a)). For Landsat 8 OLI images, a slightly different set of bands is used to conform to OLI's modified spectral range. For simplicity, bands referenced in this publication refer to Landsat 7 ETM+ spectral ranges. The ratio of TM3/TM5 (value ≥ 2), with additional spectral information from TM1 (value > 25) has been used in previous research as an effective means of delineating glacier areas (e.g., Hall et al., 1987; Hanshaw and Bookhagen, 2014) (e.g., Hall et al., 1987; Paul and Kääb, 2005; Hanshaw and Bookhagen, but is not effective in delineating debris-covered glacier areas (Figure ??2A). In our algorithm, we use a threshold of $TM3/TM5 \geq 2$ and $TM1 > 60$ to map clean glacier ice. The end result of this step is the spectrally derived glacier outlines, which are later integrated back into the workflow before statistical filtering (Figure ??) While these thresholds perform well over many scenes, using thresholds which are not tuned to specific scene conditions can generate large errors, particularly

in shadowed areas (Paul et al., 2015). Here we choose fairly conservative threshold values to ensure that we do not remove clean glacier ice. We find that increasing the TM1 threshold results in tighter classification of debris-covered glacier tongues, but also removes some areas properly classified as glacier, particularly in steep areas of the accumulation zone. Thus, we err on the side of overclassification with our delineation of clean glacier ice. The end result of this step is the spectrally-derived (clean-ice) glacier outlines, which are later integrated back into the workflow before statistical filtering (Figure 2A).

3.3 Debris-covered Ice Delineation

3.3.1 Topographic Filtering

Building on the work of Paul et al. (2004), low slope areas (between 1 and 24°) are isolated as areas where debris-covered glaciers are likely to exist (Step 2(b)). We choose the relatively high threshold of 24°, as opposed to the 12° suggested for the Himalaya (Bolch et al., 2007), the 15° suggested for the Himachal Himalaya (Shukla et al., 2010), or the 18° suggested for the Garhwal Himalaya (Bhambri et al., 2011) to ensure that we do not prematurely remove debris-covered areas. As we use the low-slope areas as our initial maximum likely debris extent, a conservative slope threshold helps reduce errors of underclassification. Low-elevation areas (automatically defined on a scene-by-scene basis based on the average elevation of clean-ice areas minus 1750, generally below 2500-3000m 2500-3000 m in the study area) are then masked out to decrease processing time (Step 2(c)). These thresholding steps are performed independent of the previous, spectrally delineated, glacier outlines. In essence, this step identifies areas where there is the potential for a debris-covered glacier to exist, and are performed independently of the previous, pspectrally delineated, glacier outlines. Additional thresholding is then performed on this 'potential debris area' subset to identify debris-covered glacier areas (Figure ??2B).

Blue areas show 'Potential Debris Areas', as delineated by slopes between 1-24 degrees, with elevations below 2500m removed. Only these areas are examined in the subsequent thresholding steps, to reduce processing time and misclassification errors. SRTM hillshade underneath.

As can be seen in Figure ??2B, extensive areas which that are not glacier or glacier debris debris-covered glacier tongue are identified in this step. However, this step generally removes all greatly reduces the processing time of subsequent steps by removing pixels outside of the main glacierized areas of any scene, and allows and allowing the algorithm to work on a subset of the

image, thus reducing processing time. The next step uses a generalized velocity surface to subset the ‘potential debris area’ from this point forward.

150 3.3.2 Velocity Filtering

The Correlation Image Analysis Software (CIAS) (Kääb, 2002) tool, which uses a method of statistical image cross-correlation, is used to derive glacier velocities from Landsat Band 8 panchromatic images. This method functions by tracking individual pixels across space and time, and provides a velocity surface at the same resolution as the input datasets (15m) (Step 1(a)). The velocity surface is then upsampled using bilinear resampling to provide a consistent velocity estimate across the entire Landsat scene. We then standardized the velocity measurements to m/yr using the capture dates of the two Landsat images. As glacier velocity can change significantly throughout the year, and clean images were not available at exactly the same intervals for each ~~Path/Row~~ Path-Row combination, there is some error in our velocity fields. However, as the velocity surface is used to remove stable ground, which is generally well-defined despite changes in glacier velocities, errors in the velocity surface do not contribute significantly to glacier classification errors, excepting on slower-moving parts of debris-covered glacier tongues. It is important to note that ~~cloud images must be cloud-free over glaciers and snow-free images are essential off glaciers~~ for this step, as the presence of snow or cloud cover can disrupt the correlation process, resulting in anomalous velocity measurements. An example velocity surface is shown in Figure ??-2C (Step 2(d)). Red areas are removed from the ‘potential debris areas’, as they fall outside of the expected range of debris-tongue velocities.

~~Example of an annual glacial velocity surface, generated using Normalized Image Cross Correlation (NICC). Areas in red are slow-moving areas and represent stable ground. They are removed from the ‘potential debris areas.’~~

170 We only used one multi-year velocity measurement for each ~~path/row~~ Path-Row combination to derive general areas of movement/stability for glacier classification, as using stepped velocity measurements over smaller time increments did not show a noticeable improvement in glacier classification. This also improved our classification of slow-moving glaciers, which may not change significantly over only a single year. These velocities ranged generally from 4.5-30 m/yr across the different scenes. A single velocity threshold of 5 m/yr was used across all scenes to remove stable ground. A method of frequential cross-correlation using the co-registration of optically sensed images and correlation (COSI-Corr) tool (Leprince et al., 2007; Scherler et al., 2011b) was tested and

did not show any appreciable improvement in velocity measurements (Heid and Kääb, 2012).

The velocity step is most important for removing hard-to-classify pixels along the edges of glaciers, and wet sands in riverbeds. These regions are often spectrally indistinguishable from debris tongues, but have very different velocity profiles. It is important to note, however, that this step also removes some glacier area, as not all parts of a glacier are moving at the same speed. This can result in small holes in the delineated glaciers, which the algorithm attempts to rectify using statistical filtering. Generating a velocity field is the most computationally expensive step of the algorithm.

3.3.3 Spatial Weighting

~~Example of distance-weighting seed areas used to remove pixels from the ‘potential debris areas’ which are distant from either a river valley or classified glacier ice. Rivers in blue, spectrally-delineated glaciers are outlines in black. The blue lines illustrate the presence of river networks along debris-covered tongues of glaciers where there is little clean glacier ice.~~

After topographic and velocity filtering, a set of spatially-weighted filters was constructed. The first filtering step uses the Hydrosheds river network to remove ‘potential debris areas’ which are distant from the center of a given glacier valley (Figure ??2D, Step 2(e)). As glaciers occur along the flowlines of rivers, and the Hydrosheds river network generally delineates flowlines nearly to the peaks of mountains, the river network provides an ideal set of seed points with which to remove misclassified pixels outside of river valleys. A second distance weighting is then performed using the clean-ice outlines generated in Step 2(a), as well as any manual seed points provided (Step 2(f)). As debris tongues must occur in proximity to either glacier areas or the centerlines of valleys, these two steps are effective in removing overclassified areas (Figure ??)—2D). The spatial weighting performed here differs from that proposed by Paul et al. (2004) in that it uses a measure of geodesic distance from given seed points, as opposed to maintaining entire polygons which are connected to clean-ice areas. This difference helps remove non-glacier areas that are distant from clean ice, but still connected by at least a single pixel to clean-ice areas. At this step, it is possible to add manual seed points, which may be necessary for some longer debris tongues. We note that these are optional, and the majority of glaciers do not need the addition of manual seed points. However, for certain irregular or cirque glaciers, the addition of manual seed points has been observed to increase the efficacy of the algorithm. In processing the Landsat imagery presented here, we have not used additional manual seed points.

~~Areas removed by second distance weighting step (red). The geodesic distance algorithm removes isolated areas near glaciers as well as areas distant from any glacier.~~

210 The spatial weighting step is essential for removing pixels spatially distant from any clean-ice area. In many cases, large numbers of river pixels, and in some cases, dry sand pixels, have similar spectral and topographic profiles to debris covered glaciers. This step effectively removes the majority of pixels outside the general ~~glaciated glacierized~~ area(s) of a Landsat scene, as can be seen in Figure ??2E.

215 3.3.4 Statistical Filtering

Once the spatial weighting steps are completed, a set of three filters are then applied, in order to remove isolated pixels, bridge gaps between isolated glacier areas, and fill holes in large contiguous areas (Step 2(g)). First, a 3x3 median filter is applied, followed by an 'area opening' filter, which fills holes in contiguous glacier areas. Finally, an 'image bridging' filter is applied to connect disjointed
220 areas, and fill holes missed by the area opening filter.

This step is ~~essential necessary~~ for filling holes and reconnecting separated glacier areas. ~~As our initial filtering methods are based on a fixed set of threshold values, there are often glacier pixels which are removed that result from the initial threshold-based filtering steps.~~ For example, some slow-moving pixels in the middle of a debris tongue may be moving more slowly than the provided
225 velocity threshold, and are thus removed. This problem is somewhat, but not completely, mitigated ~~debris-covered glacier tongue that were removed based on velocity filtering are often restored by the statistical filtering (Figure ??).~~

~~Final algorithm outlines (black) with areas classified after the clean-ice delineation in red. Illustrates the improved classification by the algorithm across several large debris tongues. Landsat OLI image captured Sept 25, 2013 as background.~~
230

3). The improved classification of debris areas between the clean-ice and final algorithm outputs can clearly be seen in Figure ??3.

3.4 Creation of Manual Control Datasets

Manual control datasets encompassing ~750 glaciers (~11,000 km²) were created to test the efficacy of the glacier mapping algorithm. These datasets were digitized ~~off of~~ from Landsat imagery in
235 a GIS, and then corrected with higher resolution imagery in Google Earth. The datasets are coherent

in space, but cover two different times (~ 2000 and ~ 2011 , depending on the dates of the available Landsat scenes). The bulk of the manually digitized glaciers fall within the boundary of Landsat ~~Path/Row~~Path-Row combination 147/031, as this is the most heavily glacierized sub-region of our study area. However, we have digitized glaciers throughout the eight ~~Path/Row~~Path-Row combinations to avoid biasing our statistics and algorithm to one specific scene extent. We have also considered a wide range of size classes in our manual dataset ($<0.5 \text{ km}^2$ to $500+ \text{ km}^2$), as well as both ~~clean~~clean-ice and debris-covered glaciers. We note that although the manual datasets here are considered ‘perfect’, there is inherent error in any manual digitization in a GIS (e.g., Paul et al., 2013). Due to the lack of ground truth information, we have estimated the overall uncertainty of the manual dataset to be 2% based on previous experiments (Paul et al., 2002, 2013). Figure 4 shows the ~~size-class~~size-class distribution of the manual control dataset, with logarithmic area scaling.

Before any comparisons between glaciers can be performed, glacier complexes must be split into component parts. A set of manually edited watershed boundaries, derived from the SRTM DEM, were used to split both the manual and algorithm datasets into individual glacier areas for analysis. In this way, the diverse datasets and classified glacier areas can be split into the same subset areas for statistical comparison.

4 Results

Over the eight Landsat footprints used in this study, we map $\sim 44,000 \text{ km}^2$ of glaciers over a two distinct time slices. Several additional time periods were mapped, but not included in the statistical analysis presented in this manuscript.

4.1 Statistical Analysis of Algorithm Errors

A subset of 215 glaciers from the manual control datasets of varying size and topographic setting was chosen for more detailed analysis. The unedited, algorithm-generated, glacier outlines were compared against spectral outlines, which only classify the glacier areas via commonly used spectral subsetting (using TM1, TM3, and TM5, produced in Step 2(b)), the manual control datasets, and the CGI v2. Figure ??-5A shows the bulk elevation distributions across 215 glaciers for each dataset in ~~10m~~10 m elevation bins.

There is some apparent bias in our algorithm towards ~~low-elevation~~low-elevation areas, which represent the debris-covered portions of glaciers and are the most difficult areas to classify. This

bias also stems from misclassified areas in shadows, particularly in north-facing glaciers. There is also a bias in our control dataset towards underclassifying the ~~high-elevation-high-elevation~~ areas, which we attribute to user bias in removing isolated rock outcrops within glaciers, as opposed to simply defining accumulation areas as a single polygon. In general, the algorithm and the control dataset are ~~well-matched~~ well-matched below 4000 meters; above this, the spectral dataset and the algorithm dataset begin to align closely and generally follow the manually digitized data. This threshold represents the general transition from debris-covered glaciers to clean glacier ice in the study area. Our algorithm output is also well-matched with the CGI v2, except at very high elevations where it overclassifies some areas as compared to the CGI v2.

Elevation distributions of over- and under-classified glacier areas, as compared to a manual control dataset ($n=75,330 \text{ km}^2$). Overclassified areas show that the algorithm does not remove large portions of the accumulation area, but instead adds additional area as compared to the control dataset. Underclassified areas indicate that the algorithm identifies less area than the manually digitized dataset in low-elevation regions. 5.5 is overclassified, and 0.8 is underclassified.

In order to examine inherent bias throughout the algorithm classification, under- and over-classified areas ~~were examined~~ were examined for a subset of the control dataset. To determine areas of over-classification (underclassification), the manually (algorithm) generated dataset was subtracted from the algorithm (manual) dataset, leaving only pixels ~~which are that were~~ which are that were overclassified (underclassified). Figure ??-5B shows the elevation distributions of under and over classified areas. The algorithm tends to consistently overclassify areas across the range of glacier elevations, which we attribute here to differences in manual and algorithm treatment of steep and ~~de-glaciated-de-glacierized~~ areas within glacier accumulation zones. Importantly, the algorithm underclassifies a much smaller number of pixels, generally corresponding to areas below ~~4000m~~ 4000 m, where debris tongues are dominant. The majority of these pixels are along the edges of ~~glacier debris-debris-covered glacier~~ tongues, which are removed by the algorithm due to their low relative velocity. It is also possible that some of these pixels are ‘dead ice’, which is difficult to differentiate from debris tongues by visual inspection. The total misclassification of algorithm-derived outlines against two independent manual control datasets ~~are is~~ is 2% and 10% respectively, which represents a significant improvement from a pure spectral delineation approach.

To investigate sampling bias in our analysis, we used 465 GLIMS glacier identification numbers (centroids, point features) ~~which that~~ which that overlapped with the manual control datasets. A random sub-

set of 100 of these points was chosen for this analysis. As can be seen in Figure 225C, similar patterns emerge between the randomly sampled glaciers and the sampling used in other sections of this manuscript. There is evidence of more noise in the random sample, as some glaciers which we avoided due to closeness to wet sand/or other hard-to-classify areas were chosen during the random sampling. However, the relationship between the algorithm and the manual datasets remains significant (Kolmogorov–Smirnov test passes at 99% confidence interval).

~~Averaged elevation differences for a random sample of glaciers overlapping a manual control dataset (n=100, 100 km²). Shows generally close agreement between the manual glacier dataset and the algorithm dataset below 4000m, with closer agreement between the spectral and algorithm datasets above 4000m. This indicates improved mapping of debris-tongues by the algorithm, and similar treatment of clean ice by both the algorithm and the spectrally-delineated glaciers.~~

4.2 Vertex Distance Matching

To capture changes in the shape of the glacier outlines between the initial spectral classification and the final algorithm output, we computed the distance between pairs of glacier vertices. We first reduced our manual control dataset to ~~component vertices~~ a set of X/Y pairs for each component vertex, which were then matched to the closest vertex in the spectral and final algorithm ~~results~~ result's polygons, respectively. ~~The results of this distance matching can be seen in Figure 6(Figure 6).~~

The distance distribution for the algorithm dataset shows generally close agreement between the algorithm and manual control datasets. The spectral dataset also contains a large percentage of vertices close to a 1:1 agreement with the manual control dataset, which are primarily those vertices at the upper edges of glaciers, or vertices from small, debris-free glaciers. The difference in these two distributions is attributed to the increased precision with which the algorithm maps debris-covered glacier outlines. Both datasets were normalized by their whole-dataset maximum distances.

5 Discussion

5.1 Comparison with Previous Glacier Mapping Algorithms

Several authors have presented alternative debris-covered glacier classification methods and schemes (e.g., Tasehner and Ranzi, 2002; Paul et al., 2004; Bolch et al., 2007; Shukla et al., 2010; Racoviteanu and Williams, 2012; Rastner

thermal and spectral data (Taschner and Ranzi, 2002) , topographic and neighborhood analysis (Paul et al., 2004) , clustering of optical and thermal data (Bolch et al., 2007) , maximum likelihood classification (Shukla et al., 2010) , slope and curvature clustering combined with thermal data (Bhambri et al., 2011) , decision tree classification and texture analysis, (Racoviteanu and Williams, 2012) and object-based classifications (Rastner et al., 2014) . While all of these methods present improvements over basic clean-ice delineation as proposed by Hall et al. (1987), they each have shortcomings which limit their range of use. Table 2 shows a comparison of these different methods alongside the algorithm presented in this study.

Our study improves on previous work in three main ways: (1) reduced computational intensity, (2) greater diversity of study area, and (3) increased temporal range of our dataset. The methods proposed in this study, excepting the generation of a velocity field, require very little processing power. Once initial input datasets (velocity surface, rasterized river network) have been created, a Landsat scene can be processed in 3-5 minutes (Ubuntu 14.04, 8 cores (3.6GhZ), 16 GB RAM). When this is compared with the training dataset creation, computationally expensive classification schemes, and neighborhood analyses employed by other studies, there is a clear improvement in efficiency. Secondly, we analyze a significantly larger glacier area than any of the previous studies, which has helped us generalize our algorithm and methods to a wide range of topographic and land-cover settings. Finally, we process a multi-year dataset, encompassing ~~62-40~~ Landsat scenes with varying landcover and ~~weather-meteorological~~ settings. This has allowed us to further generalize our algorithm to be effective beyond a single scene or small set of scenes, and to remain effective across a wide spatial and temporal range. The time-dynamic aspect of our algorithm can also ~~provide a complement to complement~~ time-static wide-area datasets, such as the RGI v4.0, the CGI v2, and the forthcoming GAMDAM datasets (Arendt et al., 2012; Guo et al., 2015; Nuimura et al., 2014). While these datasets may provide higher-quality manually digitized outlines for specific glaciers, they only provide a single snapshot in time, and are limited to a specific area of coverage.

5.2 ~~Unused-Additional Tested~~ Filtering Steps

Two additional topographic indices – spatial Fast Fourier Transforms (FFTs), also known as 2D FFTs, and ASTER surface roughness measurements – were tested during the development of the algorithm, although neither provided significant improvement. We attempted to derive frequential information from several Landsat and ASTER bands, with limited success. Some glaciers exhibit a

unique frequency signature when analyzed using spatial FFTs, although these were not consistent across multiple debris-covered glaciers with differing surface characteristics. Additionally, the FFT approach was tested against a principal component analysis (PCA) image derived from all Landsat bands, without significant improvement to the algorithm.

We also attempted to integrate surface roughness measurements using the ASTER satellite, which contains both forward looking (3N - nadir) and backwards looking (3B - backwards) images, primarily intended for the generation of stereoscopic DEMs. The difference in imaging angle provides the opportunity to examine surface roughness by examining changes in shadowed areas (Mushkin et al., 2006; Mushkin and Gillespie, 2011). We found that there are slight surface roughness differences between ~~glaciated and non-glaciated areas on some debris tongue~~terrain on and off glaciers, but that these differences are not significant enough to use as a thresholding metric. Furthermore, the nature of the steep topography limits the efficacy of this method, as valleys which lie parallel the satellite flight path and those which lie perpendicular to the flight path show different results. Thus, the algorithm relies on the velocity and slope thresholds to characterize the topography of the glacier areas.

5.3 Algorithm Use Cases and Caveats

The glacier outlines provided by the algorithm are a useful ~~first-pass~~first-pass analysis of glacier area. It is often more efficient to digitize only misclassified areas, as opposed to digitizing entire glacier areas by hand (Paul et al., 2013). Paul et al. (2013) also note that for clean ice, automatically derived glacier outlines tend to be more accurate, and it is only in the more difficult debris-covered and shadowed areas that manual digitization becomes preferable. In the algorithm presented here, clean ice thresholding was implemented using TM1, TM3, and TM5. However, because the algorithm operates primarily on 'potential debris areas', any clean ice classification scheme could be used. For example, in other study regions, or for different satellite sensors, other schemes, such as the Normalized Difference Snow Index (Dozier, 1989), may outperform clean ice classification as implemented in this study.

The algorithm moves a step further than spectral-only classification and attempts to classify glacier areas as accurately as possible, including debris-covered areas. As can be seen in Figure 7, the algorithm compares well with both the control dataset and the CGI v2 – a high-fidelity, manually edited, dataset – across a range of glacier types (Step 2(a)) (Guo et al., 2015). However, the algorithm

385 outlines do not perfectly align with either dataset. In Figure 7, a tendency to remove pixels along the
edge of ~~glacier debris~~ debris-covered glacier tongues can be observed, which we attribute to the fact
that the center of debris tongues often move faster than the edges. Furthermore, both the algorithm
results and the manual control dataset underestimate glacier area as compared to the CGI v2, due
to the removal of non-clean ice pixels at high altitudes or high slopes, which are generally within
390 the accumulation area of a glacier but are not always covered by permanent ice. These two types
of classification bias are easily rectified with minimal manual intervention. Some bias between the
manual or algorithm datasets and the CGI v2 can also be attributed to the difference in time; while
the manual and algorithm datasets share an image date, the CGI v2 was digitized on top of multiple
images that may not match up perfectly in time with our datasets. Despite these misclassified areas,
395 the raw algorithm output effectively identifies the furthest reaches of the glacier tongues ~~effectively~~
in most cases, as can be seen in three long debris tongues shown in Figure 7.

Without post-processing, these raw glacier outlines can be used to analyze regional glacier char-
acteristics, such as slope, aspect, and hypsometry. Even if glacier outlines are not perfectly recti-
fied in space, at the scale of watersheds, satellite image footprints, or mountain ranges, errors of
400 under- and over-classification even out, yielding valuable regional statistics (Figure ~~??5A~~). As the
method can be easily modified to fit the topographic and glacier setting of any region, it is a power-
ful tool for ~~analyzing~~ analysing glacier changes over large scales ~~over~~ for the period of Landsat TM,
ETM+ and OLI coverage. ~~Small~~ While the algorithm has yet to be applied to large and slow-moving
debris-covered glaciers in the Himalaya, a wide range of glacier size classes, speeds, and topographic
405 settings are well classified by the algorithm. For example, even small glacier changes are also cap-
tured by the algorithm, as can be seen in Figure 8.

Figure 8 also illustrates some potential errors ~~with-in~~ in the algorithm where river sand is sometimes
delineated as glacier area. In many cases, the same areas are captured across different timestamps,
as the topographic and velocity data used to define ‘potential debris areas’ is mostly static in time,
410 excepting the distance weighting steps. However, these areas are easily removed during manual
inspection of results.

The second use case for the algorithm is as a substitute for simple spectral ratios. ~~Particularly~~
~~in regions with numerous debris-covered glaciers, manual~~ Manual digitization of glacier tongues
is time consuming, particularly in regions with numerous debris-covered glaciers. Our algorithm
415 provides a robust baseline set of glacier outlines ~~which that~~ can be corrected manually, with mini-

mal extra processing time. As generating the input velocity surfaces can take longer than processing glacier outlines from dozens of Landsat scenes, efficiencies are gained when ~~a large number of Landsat scenes are processed in bulk.~~ The algorithm ~~as published~~ presented in this manuscript takes ~3-5 minutes of actual processing time once the base datasets have been created. For a single ~~Path/Row~~ Path-Row combination, the time to set up the input datasets (velocity surface, manual debris points) is ~4 hours. Once the initial setup has been completed for a given ~~Path/Row combination, an arbitrary Path-Row combination,~~ any number of Landsat scenes can be processed very quickly.

Although the algorithm represents a step forward in semi-automated glacier classification, there are several important caveats to keep in mind: (1) Lack of data density and temporal range limits the efficacy of individual glacier analysis; the algorithm presented in this paper was not designed with individual glacier studies in mind, and in many cases, such as in mass balance studies, more accurate manual glacier outlines are necessary. Furthermore, (2) the algorithm relies on manual intervention to separate individual glaciers which are connected through overlapping classified areas, or which are part of glacier complexes. Finally, (3) the algorithm relies heavily on the fidelity of the Landsat images provided, in that glacier outlines on images with cloud- or snow-cover are less likely to be well defined. This creates a data limitation, as many glacierized areas are subject to frequent cloud- and snow-cover, and thus have a limited number of potentially useful Landsat images for the purpose of this algorithm.

6 Conclusions

This study presents an enhanced glacier classification methodology based on the spectral, topographic, and spatial characteristics of glaciers. We present a new method of (semi-) automated glacier classification, which is built upon, but unique from, the work of previous authors. Although it does not completely solve the difficulties associated with debris-covered glaciers, it can effectively and rapidly characterize glaciers over a wide area. Following an initial delineation of clean glacier ice, a set of velocity, spatial, and statistical filters are applied to accurately delineate glacier outlines, including their debris-covered areas.

When compared visually and statistically against a manually digitized control dataset and the high-fidelity CGI v2, our algorithm remains robust across the wide range of glacier sizes and types found in ~~Northern and Central Asia.~~ The algorithm developed here ~~will be~~ is applicable to a wide range of glacierized regions, particularly in those regions where debris-covered glaciers are domi-

nant, and extensive manual digitization of glacier areas has previously been required. The raw algorithm output is usable for rough statistical queries on glacier area, hypsometry, slope, and aspect; however, manual inspection of algorithm output is necessary before using ~~algorithm~~ the generated glacier outlines for more in-depth area change or mass balance studies.

450 *Acknowledgements.* ~~This Part of this~~ work was supported through the Earth Research Institute (UCSB) through a Natural Hazards Research Fellowship, as well as the NSF grant AGS-1116105. We would like to thank Frank Paul, Wanqin Guo, and one anonymous reviewer for their detailed and helpful reviews, as well as Tobias Bolch for his contribution to the development of the manuscript.

References

- 455 Arendt, A., Bolch, T., Cogley, J., Gardner, A., Hagen, J., Hock, R., Kaser, G., Pfeffer, W., Moholdt, G., Paul, F., et al.: Randolph Glacier Inventory [v2. 0]: A Dataset of Global Glacier Outlines. Global Land Ice Measurements from Space, Boulder Colorado, USA, Digital Media, 2012.
- Armstrong, R., Raup, B., Khalsa, S., Barry, R., Kargel, J., Helm, C., and Kieffer, H.: GLIMS glacier database, National Snow and Ice Data Center, Boulder, Colorado, USA, 2005.
- 460 Bhambri, R., Bolch, T., and Chaujar, R.: Mapping of debris-covered glaciers in the Garhwal Himalayas using ASTER DEMs and thermal data, *International Journal of Remote Sensing*, 32, 8095–8119, 2011.
- Bolch, T., Buchroithner, M. F., Kunert, A., and Kamp, U.: Automated delineation of debris-covered glaciers based on ASTER data, in: *Geoinformation in Europe (Proc. of 27th EARSeI Symposium, 04-07 June 2007)*, Bozen, Italy, pp. 403–410, 2007.
- 465 Bolch, T., Peters, J., Yegorov, A., Pradhan, B., Buchroithner, M., and Blagoveshchensky, V.: Identification of potentially dangerous glacial lakes in the northern Tien Shan, *Natural Hazards*, 59, 1691–1714, 2011.
- Cannon, F., Carvalho, L., Jones, C., and Bookhagen, B.: Multi-annual variations in winter westerly disturbance activity affecting the Himalaya, *Climate Dynamics*, pp. 1–15, 2014.
- Dozier, J.: Spectral signature of alpine snow cover from the Landsat Thematic Mapper, *Remote sensing of Environment*, 28, 9–22, 1989.
- 470 Guo, W., Xu, J., Liu, S., Shangguan, D., Yao, X., Wei, J., Bao, W., Yu, P., Liu, Q., and Jiang, Z.: The second Chinese glacier inventory: data, methods and results, *Journal of Glaciology*, 226, 957–969, doi: 10.3189/2015JoG14J209, 2015.
- Hall, D., Ormsby, J., Bindshadler, R., and Siddalingaiah, H.: Characterization of snow and ice reflectance zones on glaciers using Landsat Thematic Mapper data, *Ann. Glaciol*, 9, 1–5, 1987.
- 475 Hansen, M. C. and Loveland, T. R.: A review of large area monitoring of land cover change using Landsat data, *Remote sensing of Environment*, 122, 66–74, 2012.
- Hanshaw, M. and Bookhagen, B.: Glacial areas, lake areas, and snow lines from 1975 to 2012: status of the Cordillera Vilcanota, including the Quelccaya Ice Cap, northern central Andes, Peru, *The Cryosphere*, 8, 359, 2014.
- 480 Heid, T. and Kääb, A.: Evaluation of existing image matching methods for deriving glacier surface displacements globally from optical satellite imagery, *Remote Sensing of Environment*, 118, 339–355, 2012.
- Jarvis, A., Reuter, H. I., Nelson, A., Guevara, E., et al.: Hole-filled SRTM for the globe Version 4, available from the CGIAR-CSI SRTM 90m Database (<http://srtm.csi.cgiar.org>), 2008.
- 485 Kääb, A.: Monitoring high-mountain terrain deformation from repeated air- and spaceborne optical data: examples using digital aerial imagery and ASTER data, *ISPRS Journal of Photogrammetry and remote sensing*, 57, 39–52, 2002.
- Lehner, B., Verdin, K., and Jarvis, A.: New global hydrography derived from spaceborne elevation data, *EOS, Transactions American Geophysical Union*, 89, 93–94, 2008.
- 490 Leprince, S., Ayoub, F., Klingert, Y., and Avouac, J.-P.: Co-registration of optically sensed images and correlation (COSI-Corr): An operational methodology for ground deformation measurements, in: *Geoscience and Remote Sensing Symposium, 2007. IGARSS 2007. IEEE International*, pp. 1943–1946, IEEE, 2007.
- Lioubimtseva, E. and Henebry, G. M.: Climate and environmental change in arid Central Asia: Impacts, vulnerability, and adaptations, *Journal of Arid Environments*, 73, 963–977, 2009.
- 495 Mushkin, A. and Gillespie, A.: Using ASTER Stereo Images to Quantify Surface Roughness, in: *Land Remote Sensing and Global Environmental Change*, pp. 463–481, Springer, 2011.
- Mushkin, A., Gillespie, A., Danilina, I., O’Neal, M., Pietro, L., Abbott, E., and Balick, L.: Using sub-pixel roughness estimates from ASTER stereo images to compensate for roughness effects in the thermal infrared, in: *RAQRS II: 2nd International Symposium on Recent Advances in Quantitative Remote Sensing*, 2006.
- 500 Narama, C., Kääb, A., Duishonakunov, M., and Abdrakhmatov, K.: Spatial variability of recent glacier area changes in the Tien Shan Mountains, Central Asia, using Corona (~ 1970), Landsat (~ 2000), and ALOS (~ 2007) satellite data, *Global and Planetary Change*, 71, 42–54, 2010.
- Nuimura, T., Sakai, A., Taniguchi, K., Nagai, H., Lamsal, D., Tsutaki, S., Kozawa, A., Hoshina, Y., Takenaka, S., Omiya, S., et al.: The GAMDAM Glacier Inventory: a quality controlled inventory of Asian glaciers, *The Cryosphere Discussions*, 8, 2799–2829, 2014.
- 505 Paul, F.: Changes in glacier area in Tyrol, Austria, between 1969 and 1992 derived from Landsat 5 Thematic Mapper and Austrian Glacier Inventory data, *International Journal of Remote Sensing*, 23, 787–799, 2002.
- Paul, F. and Kääb, A.: Perspectives on the production of a glacier inventory from multispectral satellite data in Arctic Canada: Cumberland Peninsula, Baffin Island, *Annals of Glaciology*, 42, 59–66, 2005.

- 510 Paul, F., Kääb, A., Maisch, M., Kellenberger, T., and Haerberli, W.: The new remote-sensing-derived Swiss glacier inventory: I. Methods, *Annals of Glaciology*, 34, 355–361, 2002.
- Paul, F., Huggel, C., and Kääb, A.: Combining satellite multispectral image data and a digital elevation model for mapping debris-covered glaciers, *Remote Sensing of Environment*, 89, 510–518, 2004.
- Paul, F., Barrand, N., Baumann, S., Berthier, E., Bolch, T., Casey, K., Frey, H., Joshi, S., Konovalov, V., Le Bris, R., et al.: On the accuracy of glacier outlines derived from remote-sensing data, *Annals of Glaciology*, 54, 171–182, 2013.
- Paul, F., Bolch, T., Kääb, A., Nagler, T., Nuth, C., Scharrer, K., Shepherd, A., Strozzi, T., Ticconi, F., Bhambri, R., et al.: The glaciers climate change initiative: Methods for creating glacier area, elevation change and velocity products, *Remote Sensing of Environment*, 162, 408–426, 2015.
- 520 Pfeffer, W. T., Arendt, A., Bliss, A., Bolch, T., Cogley, J., Gardner, A., Hagen, J., Hock, R., Kaser, G., Kienholz, C., Miles, E., Moholdt, G., Mölg, Paul, F., Radić, V., Rastner, P., Raup, B., Rich, J., Sharp, M., and Consortium, T. R.: The Randolph Glacier Inventory: a globally complete inventory of glaciers, *Journal of Glaciology*, 60, 537–552, 2014.
- Racoviteanu, A. and Williams, M. W.: Decision tree and texture analysis for mapping debris-covered glaciers in the Kangchenjunga area, Eastern Himalaya, *Remote Sensing*, 4, 3078–3109, 2012.
- 525 Racoviteanu, A. E., Arnaud, Y., Williams, M. W., and Ordonez, J.: Decadal changes in glacier parameters in the Cordillera Blanca, Peru, derived from remote sensing, *Journal of Glaciology*, 54, 499–510, 2008a.
- Racoviteanu, A. E., Williams, M. W., and Barry, R. G.: Optical remote sensing of glacier characteristics: a review with focus on the Himalaya, *Sensors*, 8, 3355–3383, 2008b.
- 530 Racoviteanu, A. E., Paul, F., Raup, B., Khalsa, S. J. S., and Armstrong, R.: Challenges and recommendations in mapping of glacier parameters from space: results of the 2008 Global Land Ice Measurements from Space (GLIMS) workshop, Boulder, Colorado, USA, *Annals of Glaciology*, 50, 53–69, 2009.
- Rastner, P., Bolch, T., Notarnicola, C., and Paul, F.: A comparison of pixel-and object-based glacier classification with optical satellite images, *IEEE Journal of Selected Topics in Applied Earth Observations and Remote Sensing*, 7, 853–862, 2014.
- 535 Raup, B., Kääb, A., Kargel, J. S., Bishop, M. P., Hamilton, G., Lee, E., Paul, F., Rau, F., Soltesz, D., Khalsa, S. J. S., et al.: Remote sensing and GIS technology in the Global Land Ice Measurements from Space (GLIMS) project, *Computers & Geosciences*, 33, 104–125, 2007.
- Raup, B. H., Khalsa, S. J. S., Armstrong, R. L., Sneed, W. A., Hamilton, G. S., Paul, F., Cawkwell, F., Beedle, M. J., Menounos, B. P., Wheate, R. D., et al.: Quality in the GLIMS Glacier Database, in: *Global Land Ice Measurements from Space*, pp. 163–182, Springer, 2014.
- 540 Scherler, D., Bookhagen, B., and Strecker, M. R.: Spatially variable response of Himalayan glaciers to climate change affected by debris cover, *Nature Geoscience*, 4, 156–159, 2011a.
- Scherler, D., Bookhagen, B., and Strecker, M. R.: Hillslope-glacier coupling: The interplay of topography and glacial dynamics in High Asia, *Journal of Geophysical Research: Earth Surface*, 116, 2011b.
- 545 Shanguan, D., Bolch, T., Ding, Y., Kröhnert, M., Pieczonka, T., Wetzel, H., and Liu, S.: Mass changes of Southern and Northern Inylchek Glacier, Central Tian Shan, Kyrgyzstan, during 1975 and 2007 derived from remote sensing data, *The Cryosphere*, 9, 703–717, 2015.
- Shukla, A., Arora, M., and Gupta, R.: Synergistic approach for mapping debris-covered glaciers using optical–thermal remote sensing data with inputs from geomorphometric parameters, *Remote Sensing of Environment*, 114, 1378–1387, 2010.
- 550 Sorg, A., Bolch, T., Stoffel, M., Solomina, O., and Beniston, M.: Climate change impacts on glaciers and runoff in Tien Shan (Central Asia), *Nature Climate Change*, 2, 725–731, 2012.
- Taschner, S. and Ranzi, R.: Comparing the opportunities of Landsat-TM and Aster data for monitoring a debris covered glacier in the Italian Alps within the GLIMS project, in: *Geoscience and Remote Sensing Symposium, 2002. IGARSS’02. 2002 IEEE International*, vol. 2, pp. 1044–1046, IEEE, 2002.
- 555 Vaughan, D., Comiso, J., Allison, I., Carrasco, J., Kaser, G., Kwok, R., Mote, P., Murray, T., Paul, F., Ren, J., Rignot, E., Solomina, O., Steffen, K., and Zhang, T.: Observations: Cryosphere. In: *Climate Change 2013: The Physical Science Basis*, Contribution of Working Group I to the Fifth Assessment Report of the IPCC., 2013.
- 560

Table 1. Data table listing Landsat ~~capture~~ acquisition dates used in this study. Organized by WRS2 Path/Row combinations. Starred dates denote ‘Master’ images to which others were rectified. Bold dates indicate images used for velocity profiles.

Number of Images	144/030	145/030
Date Range of Images	11-5	10-4
LT5 Capture Acquisition Dates	2002-2013	1998-2013
	Jul 31, 2006-Sep 27, 1998	Sep 2, 1998*-1998
	Aug 8, 2009-	Oct 4, 1998-Sep 6, 2011
	Sep 27, 1998-	Jul 22, 2006-Aug 10, 2007
	Jul 13, 2011-	Aug 10, 2007
		Sep 11, 2007-
		Oct 2, 2009-
Aug 2, 2010 Jul 4, 2011 Sep 6, 2011 LE7 Capture Acquisition Dates	Sep 14, 2002*2002	
	Jul-Aug 7, 2000	
	Aug 8, 2000-	
	Jun 7, 2001-	
LC8 Capture Acquisition Dates	Oct 22, 2013	Sep 27, 2013
	Aug 19-Sep 4, 2013	
	Sep 4, 2013-	
Projection	WGS 1984 45N	
Comments	Eastern Edge of Study Area	
Number of Images	148/031	149/031
Date Range of Images	13-5	3
LT5 Capture Acquisition Dates	2002-2013	1999-2013
	Sep 16, 2007-Aug 22, 1998	Sep 7, 2007
	Sep 11, 2011	
LE7 Capture Acquisition Dates	Jul 24, 2002*2002	Sep 9, 1999* Aug 20, 2001
	Sep 18, 1999	
Aug 25, 2002 LC8 Capture Acquisition Dates	Jul 30, 2013	Oct 9, 2013
Oct 2, 2013 May 14, 2014 Projection	WGS 1984 44N	WGS 1984 43N
Comments		
Number of Images	151/033	153/033
Date Range of Images	5-4	3
LT5 Capture Acquisition Dates	1998-2013	1998-2013
Sep 10, 2009 LE7 Capture Dates	Sep 28, 1998	Sep 26, 1998
	Aug 24, 2000*-2000	Sep 29, 2002*2002
	Sep 28, 2001	
LC8 Capture Acquisition Dates	Oct 7, 2013	Oct 5, 2013
Projection	WGS 1984 43N	WGS 1984 42N
Comments		Towards Pamir Knot

Table 2. Comparison of methods between previous debris-covered glacier mapping studies.

Method	Short Description	Data Inputs	Processing Steps	Intensive	Area Covered in Study	Reported Accuracy
Taschner and Ranzi (2002)	Clean-ice detection using Landsat, coupled with ASTER thermal data	Landsat, ASTER	Data resampling, pixel clustering		5.58 km ² , Italian Alps	Not Reported
Paul et al. (2004)	Clean-ice detection using Landsat, coupled topographic analysis and neighborhood analysis	Landsat, ASTER-DEM	Image Growing Polygon neighborhood analysis		23 km ² , Swiss Alps	21% of debris misclassified
Bolch et al. (2007)	A set of training areas based on spectral and topographic information is used to determine classification thresholds	ASTER, ASTER-DEM	Creation and tuning of training dataset		Not reported, Mt. Everest Region	5% total area misclassified
Shukla et al. (2010)	Multiple landcover types mapped using spectral and thermal imagery combined with a DEM	ASTER, AWiFS, DEM	Data conversion and registration, solar illumination analysis, training dataset creation, Maximum Likelihood Classifier		200 km ² , Samudra Tapu glacier, Himachal Pradesh, India	8-14% debris misclassified
Bhambri et al. (2011)	Combination of slope and curvature data analyzed with a clustering algorithm coupled with thermal band thresholding	ASTER, DEM, Landsat, IRS PAN	Manual decisions on glacier slope and curvature clusters		232 km ² , Gongotri Glacier, Garhwal Himalaya, India	0.5-11% debris misclassified
Racoviteanu and Williams (2012)	(1) Decision tree classification with ASTER and topographic data, and (2) texture analysis exploiting surface roughness	ASTER, DEM, Quickbird, Worldview2	Training dataset creation, decision tree set-up, principal component analysis		576.4 km ² , Sikkim Himalaya, NE India	(1) 25%, (2) 31% debris misclassified
Rastner et al. (2014)	Comparison of object- and pixel-based methods of glacier mapping. Both methods use spectral and topographic information as inputs	ASTER, Landsat, DEM	Manual threshold definitions, segmentation processing, iterative thresholding		Not reported, three distinct test regions	11.5% (object-based) and 23.4% (pixel-based) misclassified areas for Himalaya region
This Study	Clean-ice detection coupled with topographic, velocity, and distance weighting thresholds	Landsat, SRTM DEM, River Network	Velocity field calculation, optional debris seed point selection		~44,000 km ² , Pamir-Tien Shan	2-10% total area misclassified

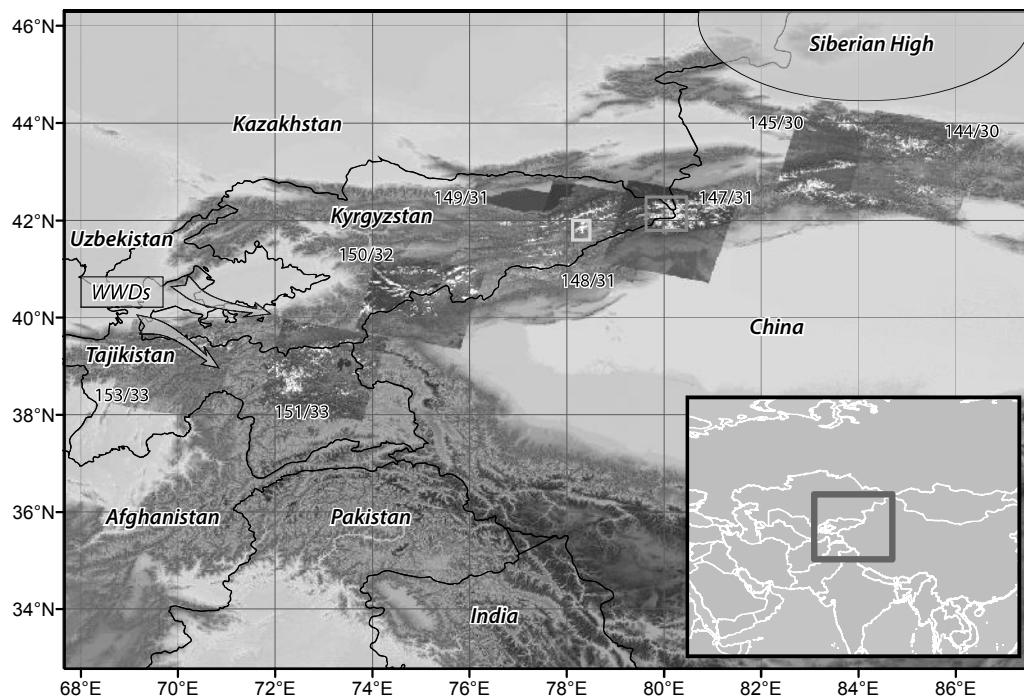


Fig. 1. Greater study area of the Tien Shan, showing SRTM v4.1 topography (Jarvis et al., 2008) and location of eight Landsat image footprints (grayscale) used in the study, along with their Path/Row combinations. Blue box delineates Figures 2-3 and 7, yellow box delineates Figure 8. Winter Westerly Disturbances and Siberian High highlighted in orange.

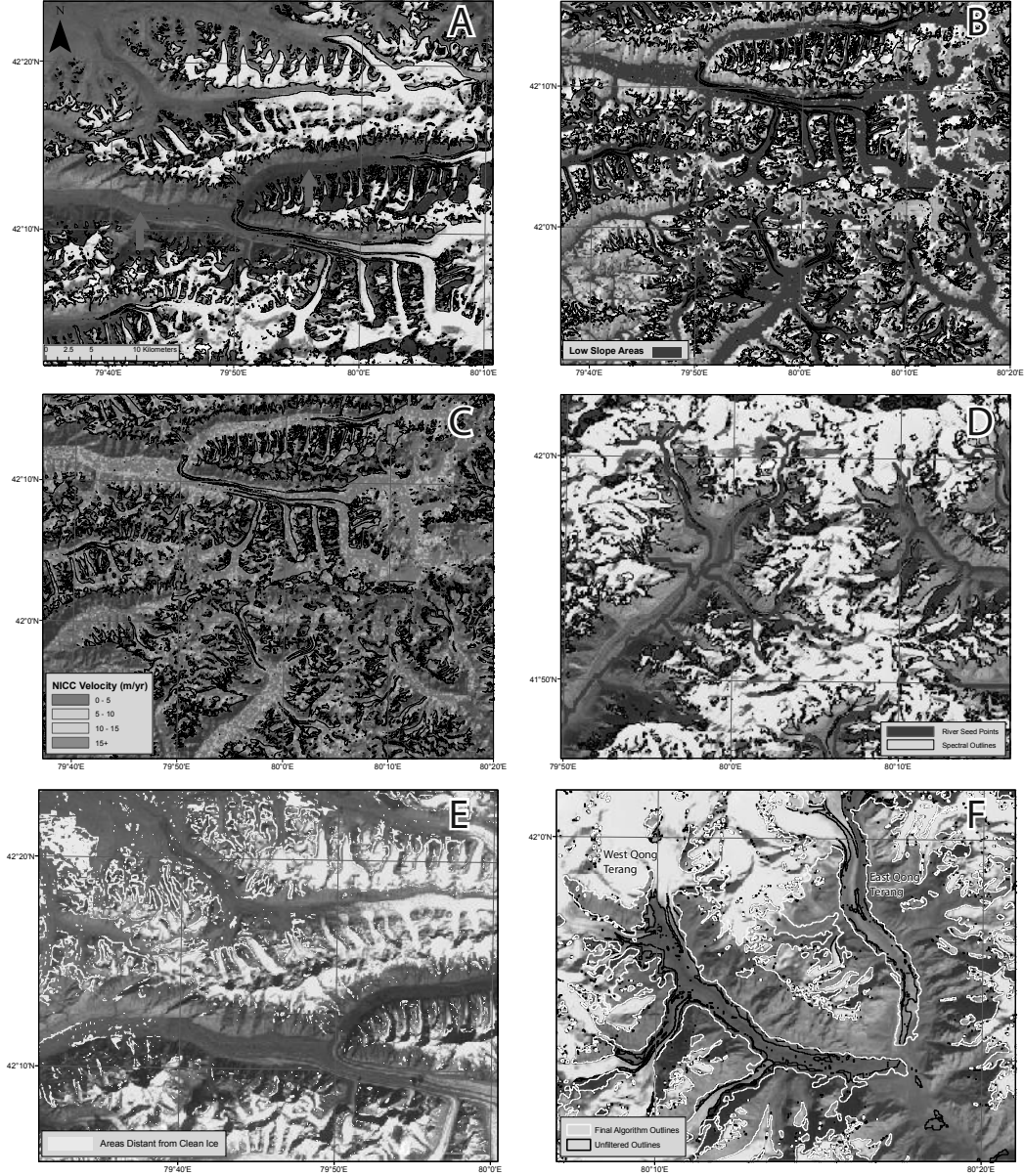


Fig. 2. (A) Characteristic example of a debris-covered glacier tongue (Inylchek Glacier). Spectrally-delineated glacier outlines (black), over Landsat bands B7/B5/B3 (R/G/B), from image LC81470312013268LGN00, with poorly mapped debris-covered tongues (red arrows). This shows generally well-mapped clean-ice (B) Blue areas show 'Potential Debris Areas', as delineated by slopes between 1-24 degrees, with elevations below ~2500 m removed, SRTM hillshade underneath, clean-ice outlines overlain in black. (C) Example of a glacier velocity surface, generated using Normalized Image Cross Correlation (NICC). Areas in red are slow-moving areas and represent stable ground, clean-ice outlines overlain in black. (D) Example of distance-weighting seed areas used to remove pixels from the 'potential debris areas' which are distant from either a river valley or classified glacier ice. Rivers in blue, but poor treatment clean-ice outlines overlain in black. (E) Areas removed by second distance weighting step (yellow). (F) Impacts of debris-covered tongues on glacier outlines, with areas in black removed during the filtering process. East and West Qong Terang Glaciers.

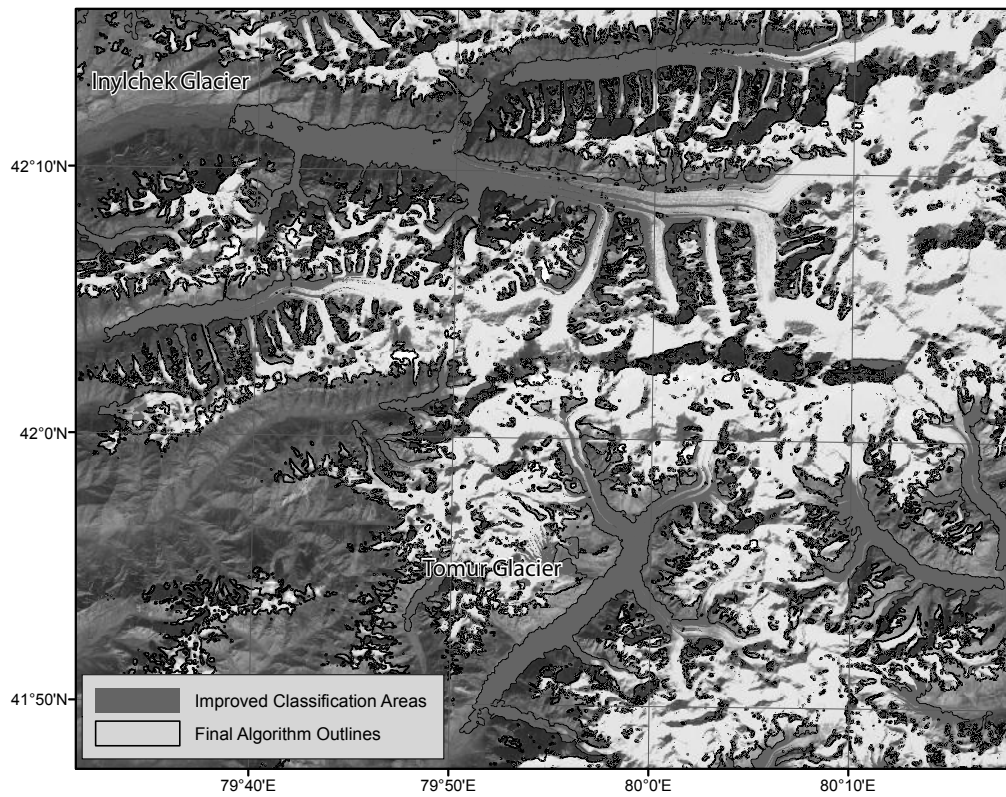
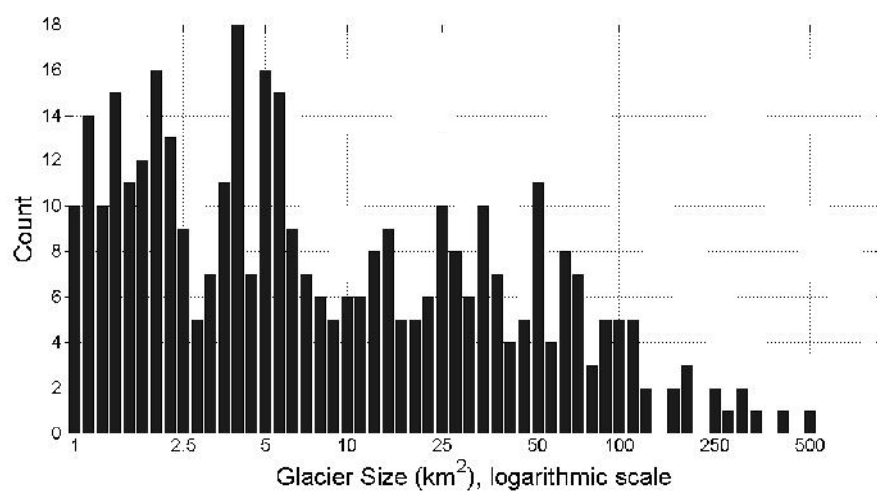


Fig. 3. Impacts of statistical filtering on glacier Final algorithm outlines (black) with areas classified in black removed during addition to the filtering process. Primarily small holes clean-ice delineation in large debris-tongues are removed, while the glacier outlines remain intact during this step. East and West Qong Terang Glaciers Landsat OLI image captured Sept 25, 2013 as background.



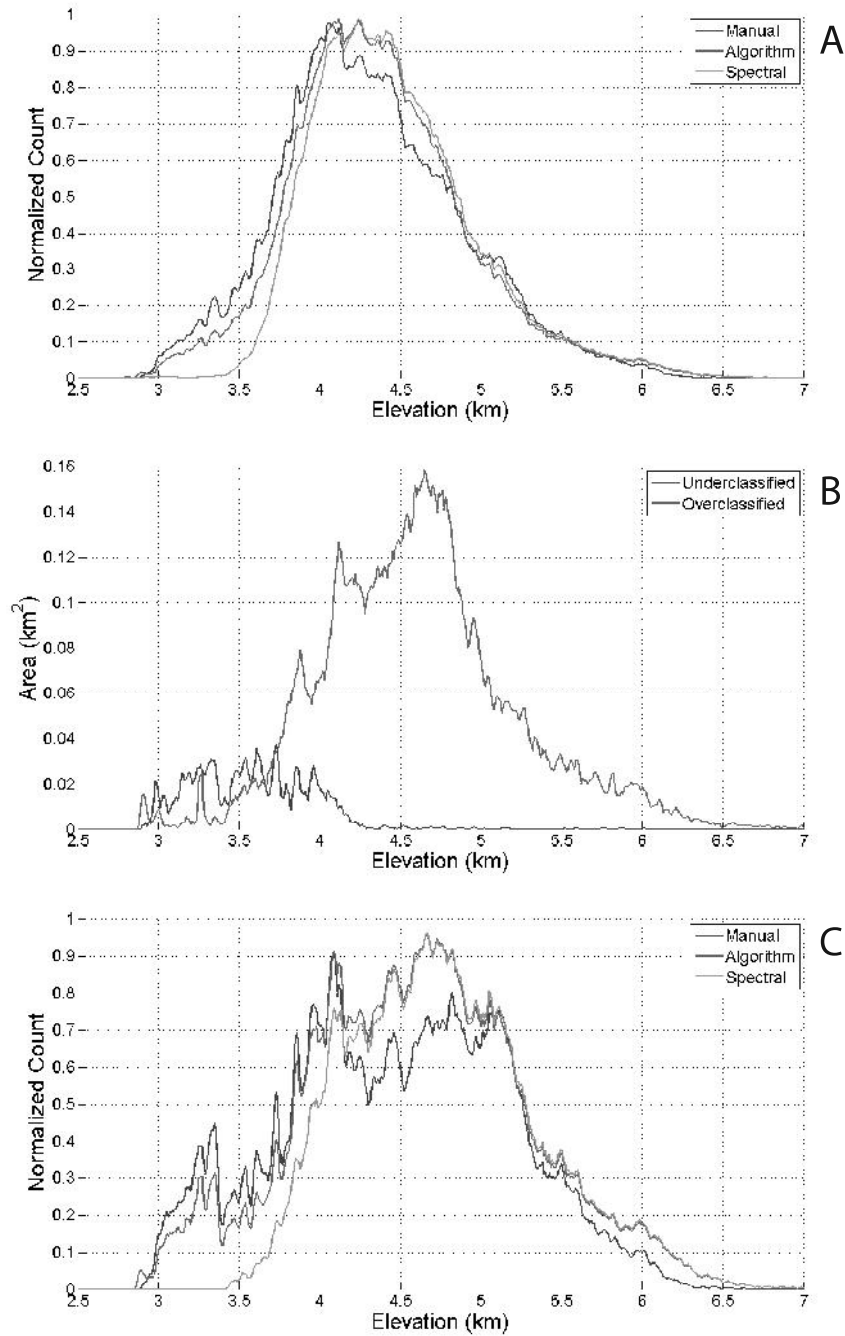


Fig. 5. (A) Bulk elevation distributions of sampled glaciers, with manual delineation (reference dataset, $n=215$, $4,500 \text{ km}^2$) in blue, algorithm-derived delineation in red, spectral delineation in green, and CGI v2 in black. Values have been normalized to maximum probability. (B) Elevation distributions of over- and under-classified glacier areas, as compared to a manual control dataset ($n=75$, 330 km^2). 5.5% is overclassified, and 0.8% is underclassified. (C) Averaged elevation differences for a random sample of glaciers overlapping a manual control dataset ($n=100$, 100 km^2).

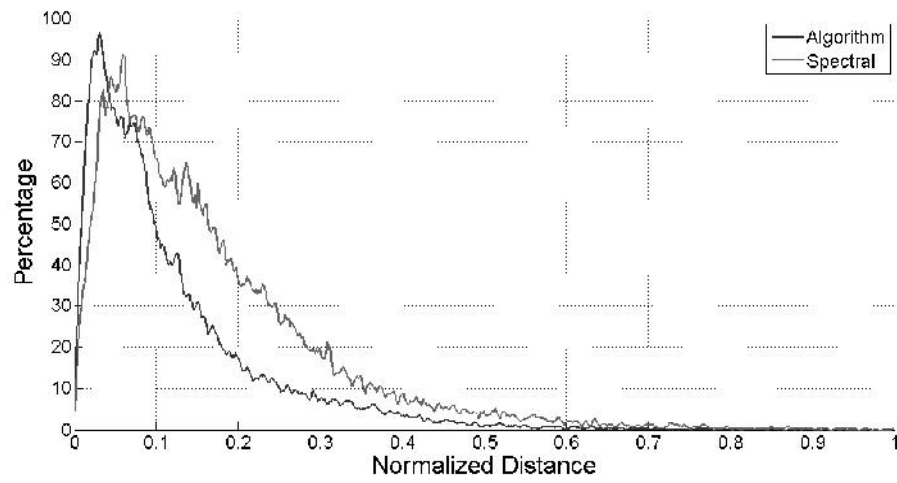


Fig. 6. Vertex distance distributions for algorithm (blue) and spectral (red) vertices, as compared to a manual control dataset, normalized to the maximum distance. This indicates generally closer agreement between the algorithm and manual datasets than between the spectral and manual datasets.

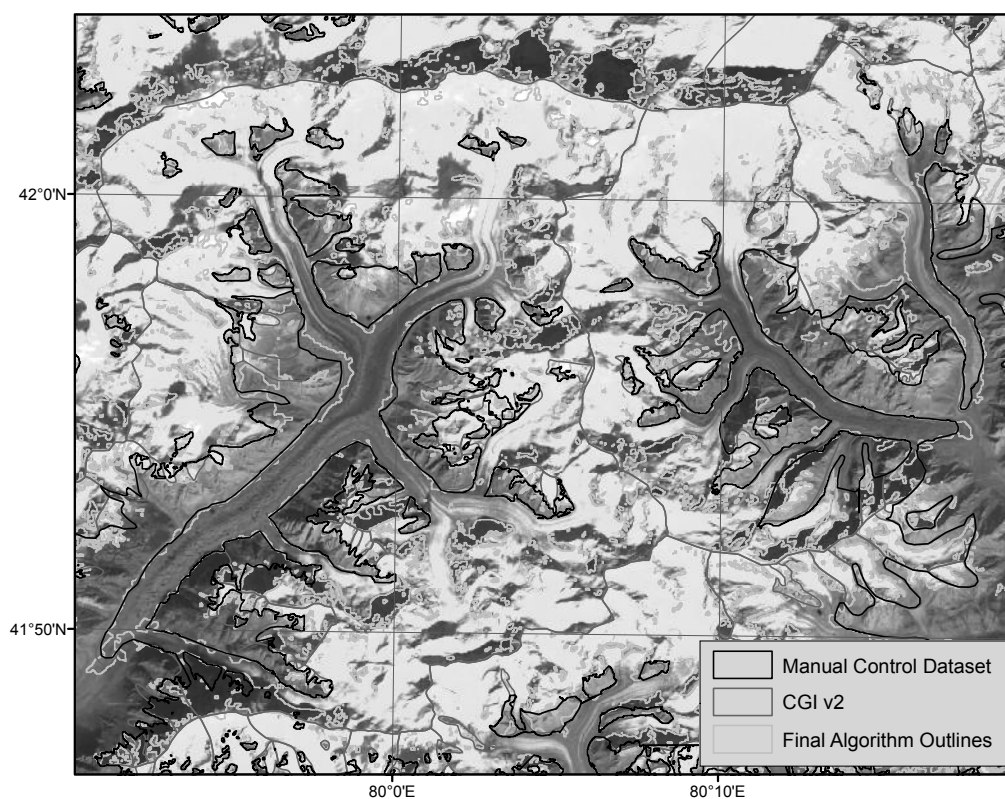


Fig. 7. Algorithm outlines (purple/yellow) compared to the control dataset (black) and the CGI v2 (red). Illustrates high fidelity in overall debris-tongue length between the three datasets, although the algorithm outlines exhibit noise along the edges of debris tongues.

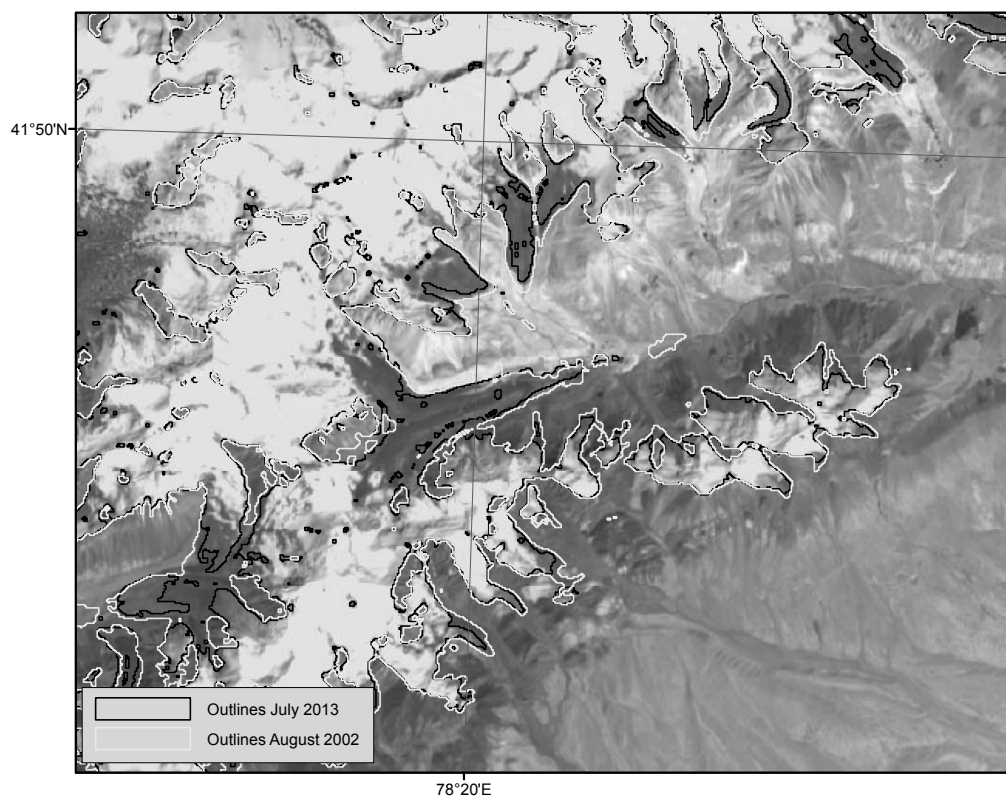


Fig. 8. Algorithm outlines for July 2013 (black) and algorithm outlines for August 2002 (red), showing small retreats in glacier areas, particularly at the debris tongues. Vicinity of the Akshiirak glacierized massif, central Tien Shan.